

# PROPAGATION METHODS FOR QUANTUM MOLECULAR DYNAMICS

*Ronnie Kosloff*

Department of Physical Chemistry and the Fritz Haber Research Center,  
The Hebrew University, Jerusalem 91904, Israel

KEYWORDS: wavepacket, Chebychev polynomial, Newtonian interpolation,  
pseudo-spectral, Krylov space

---

## INTRODUCTION

Our current understanding of molecular dynamics uses quantum mechanics as the basic underlying theory to elucidate the processes involved. Establishing numerical schemes to solve the quantum equations of motion is crucial for understanding realistic molecular encounters. The introduction of pseudo-spectral methods has been an important step in this direction. These methods allow an extremely accurate representation of the action of an operator, usually the Hamiltonian, on a wavefunction:  $\phi = \hat{H}\psi$ . A solution for the quantum molecular dynamics can be obtained by recursively applying the elementary mapping step. This recursive application of the elementary step, termed the propagator, is the subject of this review.

The natural application of a propagator is in a time-dependent description of quantum molecular dynamics, where the propagator  $\hat{U}(\tau)$  maps the wavefunction at time  $t$ ,  $\psi(t)$  to the wavefunction at time  $t + \tau$ :  $\psi(t + \tau) = \hat{U}(\tau)\psi(t)$ . The decomposition into a recursive application of the elementary step is performed by a polynomial expansion of the propagator. The introduction of the Chebychev polynomial expansion (1) first created a propagation scheme that could match the accuracy of the

pseudo-spectral elementary mapping step, thus creating a well-balanced scheme that enables highly accurate molecular dynamical calculations.

The rapid implementation of time-dependent quantum mechanical methods into molecular dynamics has been behind these developments. Just a decade ago, time-dependent quantum mechanical methods were an esoteric field shadowed by more effective time-independent approaches. Early work by McCullough & Wyatt (2, 2a) used a direct finite differencing scheme to solve the  $H + H_2$  reactive scattering problem. Now, time-dependent methods have advanced to play a major role in elucidating quantum molecular dynamics, as can be seen in two recent collections of papers (3, 4). In fact, the exponential growth of time-dependent quantum calculations makes it impossible to cover the whole field in a coherent fashion. The attempt in this review is to present only one aspect of it, the role of the propagation step.

Although the propagation step was initially designed to advance the quantum wavepacket in time, recent progress has eliminated the distinction between time-dependent and time-independent applications of propagators. For example, a propagator-based method has been developed for reactive scattering (5–10). The method is used to obtain eigenvalues, eigenfunctions (11, 12, 12a) absorption, and Raman spectra (13–15).

The polynomial expansion of the propagator can be viewed as an expansion in the Krylov vectors defined by  $\phi_n = \hat{H}^n \psi$ , where  $\hat{H}$  is the Hamiltonian of the system. The most well-known Krylov method is the Lanczos algorithm (16), introduced into molecular dynamics by Moro & Fried (17), Köppel et al (18), and Nauts & Wyatt (19, 19a). Park & Light (20) have applied the method to propagation in time (21). Since then, other Krylov-based evolution propagators have been developed (22–24). These developments have raised the issue of the relation between the Krylov-based methods and the Chebychev polynomial expansion (13). Recently, an alternative polynomial expansion based on Newton's interpolation formulas has been developed for propagating the Liouville von Neumann equation (25, 26). These developments make it extremely confusing for a casual researcher to follow the different approaches and applications; therefore, a unifying principle has to be identified that can clarify the field. This review presents an overall perspective on the different types and roles propagators play in molecular dynamics.

## THE ELEMENTARY MAPPING STEP

The starting point of a quantum molecular dynamics study is an effective scheme to represent the wavefunctions. Within this scheme, the basic mapping operation generated by an operator  $\hat{O}$  has to be defined:

$$\phi = \hat{\mathbf{O}}\psi. \quad 2.1.$$

In the pseudo-spectral approach the vectors  $\psi$  and  $\phi$  are represented on a multidimensional grid. The values of the functions at these grid points are used to generate a global functional base by matching the approximate solution to the true solution on a set of grid points:

$$\psi(x_j) = \sum_{n=0}^{N-1} a_n g_n(x_j), \quad 2.2.$$

where  $x_j$  are the grid points and  $g_n(x)$  constitute the global functional base. The pseudo-spectral scheme is based on a set of orthogonal expansion functions  $g_n(x)$  (27), which allow a direct inversion for the coefficients  $a_n$ :

$$a_n = \sum_{j=0}^{N-1} \psi(x_j) g_n^*(x_j). \quad 2.3.$$

This means that the expansion coefficients  $a_n$  are the discrete functional transform of the function  $\psi$ . Within the framework of the pseudo-spectral approach, the action of the operator  $\hat{\mathbf{O}}$  (i.e. the mapping generated by the operator,  $\phi = \hat{\mathbf{O}}\psi$ ) is handled effectively. Local operators in coordinate space, such as the potential, are calculated on the grid points while nonlocal operators, such as the kinetic energy operator, are calculated in the functional space (27). They are then recast into the same grid points. The discretization scheme determines the domain of values of the operator  $\hat{\mathbf{O}}$ . For Hermitian operators, the domain is defined by the set of eigenvalues of  $\hat{\mathbf{O}}$ . For non-Hermitian operators, the domain is defined by the range of all possible scalar products:  $\langle \psi | \hat{\mathbf{O}} | \psi \rangle / \langle \psi | \psi \rangle$ .

The use of pseudo-spectral methods is more than a technical improvement on algorithms. An elementary statement can be made that quantum mechanics is a nonlocal theory. This characteristic has to be reflected in the methods used to describe the quantum world. The foundation of the pseudo-spectral methods is, therefore, a global functional base (28); the nonlocal character of the representation is built into the formulation. The basic attributes of quantum mechanics, such as commutation relations between conjugate operators, are preserved in the pseudo-spectral description (29). Pseudo-spectral methods (28, 30–32) have exponential convergence characteristics with respect to the number of grid points or basis functions. A recent book (33) covers the basic developments of pseudo-spectral methods in the field of molecular dynamics.

## TIME PROPAGATION AND OTHER PROPAGATORS

To model the evolution of a physical system, the vector describing the state of the system has to be followed through time. In quantum mechanics

the evolution operator  $\hat{U}(t', t)$  maps the state vector at time  $t$  to a new vector at time  $t'$ . The evolution operator is constructed in compliance with the forces that induce the dynamics, which are homogeneous, symmetric and continuous in time. These requirements imply a group property to the evolution operator with the form

$$\hat{U}(t', t) = \hat{U}(t' - t) = e^{-i(\hbar)\hat{H}(t' - t)}. \quad 3.1.$$

The operator  $\hat{H}$  is a continuous generator of the evolution, and to fulfill the symmetry requirement,  $\hat{H}$  has to be Hermitian. Aside from this requirement, the operator  $\hat{H}$  is unrestricted. The operator  $\hat{H}$  is customarily identified with the Hamiltonian of the system, which means that its expectation value becomes the energy. From this analysis, one concludes that the stage on which the dynamical events are observed is the time-energy phase space. Time is interpreted as a parameter, not an operator, of a continuous dynamical group that describes the evolution operator. From this description, time and energy are apparently not on the same footing. In the position-momentum phase space, on the other hand, a complete symmetry exists between position and momentum. The difference in the descriptions is manifested in the boundary conditions. For the position-momentum space the boundary values of phase space are imposed. In the time-energy phase space only an initial boundary condition in time is imposed. The common element of both phase space descriptions is the use of global functional descriptions of the complete space. This nonlocal type of description assures the compliance with the uncertainty principles central to quantum mechanics.

The group property, which is in the foundation of the time-evolution operator  $\hat{U}$ , can be exploited by subdividing the time interval into segments:

$$\hat{U}(t+s) = \hat{U}(t)\hat{U}(s), \quad 3.2.$$

where each segment has an individual evolution operator. By repeating the segmentation process, the individual evolution operator becomes a function of a very short time interval. Knowing the limit  $\lim_{t \rightarrow 0} \hat{U}(t) = \hat{I}$ , one can linearize  $\hat{U}(t)$  for short time intervals. This is the base of a family of propagation techniques based on a short time expansion. Once a short time propagator is developed, the global evolution operator can be reassembled. Similar techniques allow the evolution operator to be developed for problems with explicit time dependence.

As a generic example, consider the time-dependent Schrödinger equation

$$i\hbar \frac{\partial \psi(t)}{\partial t} = \hat{\mathbf{H}}\psi(t), \quad 3.3.$$

subject to the initial condition  $\psi(0)$ . When the r.h.s. of the Schrödinger equation is examined, it can be identified as the elementary mapping of the vector  $\psi$ , generated by the Hamiltonian  $\hat{\mathbf{H}}$ . The discrete mapping techniques, which were discussed in the previous section, should solve the evolution of the system. For a stationary Hamiltonian, the solution of the time-dependent Schrödinger equation becomes

$$\psi(t) = e^{-(i/\hbar)\hat{\mathbf{H}}t} \psi(0). \quad 3.4.$$

This is the integral version of the time-dependent Schrödinger equation and is identical to Equation 3.3. Again comparing the r.h.s. of this integral form of the Schrödinger equation, a solution to the evolution operator is possible if a mapping procedure can be found that calculates the mapping caused by an exponential function of the Hamiltonian operator. The main topic of this review, the propagator, is thus a study of effective methods to calculate the mapping imposed on vectors in Hilbert space generated by a function of an operator. The resulting generalizations will utilize the same basic techniques developed for time evolution for solving other problems.

## FUNCTION OF AN OPERATOR

The elementary mapping step is the basis for generating the mapping of a function  $f$  of the operator  $\hat{\mathbf{O}}$ :

$$\phi = f(\hat{\mathbf{O}})\psi. \quad 4.1.$$

Using the eigenfunction equation  $\hat{\mathbf{O}}u_n = \lambda_n u_n$ , where  $\lambda_n$  is the  $n$ th eigenvalue of  $\hat{\mathbf{O}}$ , the  $n$ th projection operator is defined  $\hat{\mathbf{P}}_n = |u_n\rangle\langle u_n|$ . Using the property of the projection operators,  $\hat{\mathbf{P}}_n \hat{\mathbf{P}}_m = \delta_{nm} \hat{\mathbf{P}}_n$ , the spectral decomposition of the function of the operator in equation (4.1) can be written as

$$f(\hat{\mathbf{O}}) = \sum_n f(\lambda_n) \hat{\mathbf{P}}_n. \quad 4.2.$$

This is a key step because now the problem of evaluating a function of an operator has been transformed to the evaluation of a function of a scalar. Power expansion and spectral decomposition are the two basic methods of evaluating a function of an operator. However, the formula must perform the mapping of  $\psi$  caused by the projection operators  $\phi_n = \hat{\mathbf{P}}_n \psi$ . These operators are closely analogous to the Lagrange interpolation polynomials.

Because of the importance of these steps, a detailed description follows. First, consider the operator

$$\hat{\mathbf{Q}}_1 = (\hat{\mathbf{O}} - \lambda_1 \hat{\mathbf{I}}), \quad 4.3.$$

where  $\hat{\mathbf{I}}$  is the identity operator. This operator has the opposite effect of the projection operator, because it eliminates the component belonging to the eigenvector  $l$  from  $\psi$ . This is now the basic building block. By successively applying these operators, one can eliminate all eigenvectors except the  $n$ th one from the vector  $\psi$ . Assuming, for simplicity, that  $\hat{\mathbf{O}}$  has nondegenerate eigenvalues, a polynomial representation of the  $n$ th projection operator results:

$$\hat{\mathbf{P}}_n = \frac{1}{\mathcal{N}} \hat{\mathbf{Q}}_N \dots \hat{\mathbf{Q}}_{n+1} \hat{\mathbf{Q}}_{n-1} \dots \hat{\mathbf{Q}}_1 \hat{\mathbf{Q}}_0 = \frac{1}{\mathcal{N}} (\hat{\mathbf{O}} - \lambda_N \hat{\mathbf{I}}) \dots (\hat{\mathbf{O}} - \lambda_{n-1} \hat{\mathbf{I}}) \dots (\hat{\mathbf{O}} - \lambda_{n-1} \hat{\mathbf{I}}) (\hat{\mathbf{O}} - \lambda_{n+1} \hat{\mathbf{I}}) \dots (\hat{\mathbf{O}} - \lambda_1 \hat{\mathbf{I}}) (\hat{\mathbf{O}} - \lambda_0 \hat{\mathbf{I}}), \quad 4.4.$$

where  $\mathcal{N}$  is a normalization term that becomes

$$\mathcal{N} = (\lambda_n - \lambda_N)(\lambda_n - \lambda_{N-1}) \dots (\lambda_n - \lambda_{n-1}) \times (\lambda_n - \lambda_{n+1}) \dots (\lambda_n - \lambda_1)(\lambda_n - \lambda_0). \quad 4.5.$$

Inserting Equation 4.4 into Equation 4.2 constitutes a Lagrange interpolation procedure for evaluating the function of the operator. The polynomials can be evaluated recursively by successive application of the basic mapping of the operator in Equation 4.3. The functional evaluation is at the interpolation points, which match the eigenvalues of  $\hat{\mathbf{O}}$ . This exact reconstruction of Equation 4.2 results from the following property of interpolation polynomials:

$$\mathcal{P}_{N+1}(x_n) \equiv f(x_n). \quad 4.6.$$

Numerically, the Lagrange interpolation procedure has disadvantages because  $N$  different polynomials have to be evaluated and because numerical instability occurs.

### *Newtonian Interpolation Polynomials*

The problems can be overcome by the use of a Newtonian formulation of the interpolation polynomial,

$$f(z) \approx a_0 + a_1(z - x_0) + a_2(z - x_1)(z - x_0) + a_3(z - x_2)(z - x_1)(z - x_0) + \dots, \quad 4.7.$$

where remainder coefficients  $a_k$  are determined by imposing the interpolation condition, thus leading to

$$a_0 = f[x_0] = f(x_0)$$

and

$$a_1 = f[x_0, x_1] = \frac{f(x_1) - f(x_0)}{x_1 - x_0}. \quad 4.8.$$

The rest of the coefficients are calculated by the recursive formula

$$a_k = f[x_0, x_1, \dots, x_k] = \frac{f(x_k) - a_0 - \sum_{j=1}^{k-1} a_1(x_k - x_0) \dots (x_k - x_{j-1})}{(x_k - x_0) \dots (x_k - x_{k-1})}. \quad 4.9.$$

The coefficients  $a_k$  are called the divided difference coefficients, and a common symbol for them is  $a_k = f[x_0, x_1, \dots, x_k]$  (e.g., 34). By using the results of Equation 4.1, rewriting Equation 4.7, and replacing  $z$  with  $\hat{\mathbf{O}}$ , the function of the operator  $f$  becomes

$$\begin{aligned} f(\hat{\mathbf{O}}) &= a_0 \hat{\mathbf{I}} + a_1(\hat{\mathbf{O}} - x_0 \hat{\mathbf{I}}) + a_2(\hat{\mathbf{O}} - x_1 \hat{\mathbf{I}})(\hat{\mathbf{O}} - x_0 \hat{\mathbf{I}}) \\ &+ \dots = \sum_{n=0}^{N-1} a_n \prod_{j=0}^{n-1} \hat{\mathbf{Q}}_j = \sum_{n=0}^{N-1} a_n \prod_{j=0}^{n-1} (\hat{\mathbf{O}} - x_j \hat{\mathbf{I}}), \quad 4.10. \end{aligned}$$

where  $x_n = \lambda_n$ , and where the expansion coefficients  $a_n$  are calculated by Equations 4.8 and 4.9. This formulation leads to a recursive algorithm based on the elementary mapping. It also allows the construction of the operation of a function on an initial vector  $\psi$  once an algorithm for the mapping operation  $\hat{\mathbf{O}}\psi$  exists. This recursive algorithm eliminates intermediate storage because, unlike Equation 4.2, the need for the eigenfunctions is eliminated.

To summarize, the reformulation from Equation 4.1 to Equation 4.10 results in a finite recursive polynomial expansion of the function  $f(\hat{\mathbf{O}})$  based on the elementary mapping operation  $\hat{\mathbf{O}}\psi$ . The main advantage of the formulation in Equation 4.10 is that it separates the expansion into a sum of recursive polynomials in  $\hat{\mathbf{O}}$ , which is true for any function  $f$ . Only the expansion coefficients  $a_n$  depend on the function  $f$  through Equations 4.8 and 4.9. However, the algorithm is also based on the solution of the more difficult problem of finding the set of eigenvalues of the operator  $\hat{\mathbf{O}}$ . Because basic diagonalization procedures scale as  $O(N^3)$ , where  $N$  is the size of the vector  $\psi$ , this approach is prohibitively expensive for realistic problems.

Equation 4.10 solves the problem of the functional operation  $f(\hat{\mathbf{O}})\psi$  only formally because eventually it requires the diagonalization of the operator  $\hat{\mathbf{O}}$  in order to find the interpolation points. The next sections are

devoted to exploring the possibilities of using approximate interpolation points that will free the method from the diagonalization step. To study this possibility, one has to estimate the error introduced by relaxing the restriction that the interpolation points are equal to the eigenvalues. The advantage of the Newtonian formulation of the interpolation polynomial is that it allows a successive addition of new interpolating points. This feature will be used to obtain an estimation of the error.

### *Error Analysis*

Consider a polynomial with  $N$  interpolation points. The error at a particular point  $\xi$  is found by adding  $\xi$  as a new interpolation point leading to an  $N + 1$  interpolation polynomial. Then the error at the point  $\xi$  of the  $N$ th polynomial is equal to the added term:

$$\text{error}(\xi) = f[x_1, x_2, \dots, x_n, \dots, x_N, \xi] \prod_{j=0}^{N-1} (\xi - x_j). \quad 4.11.$$

By analogy, the error in the functional operation  $f(\hat{\mathbf{O}})$  is obtained by replacing  $\xi$  with  $\hat{\mathbf{O}}$ :

$$\text{error} = \left\| f[z_1, x_2, \dots, x_n, \dots, x_N, \hat{\mathbf{O}}] \prod_{j=0}^{N-1} \hat{\mathbf{Q}}_j \right\|. \quad 4.12.$$

The strategy of locating the interpolation points is based on minimizing the error in Equation 4.12. The error term consists of a product of two terms: the divided difference term and the product term. The divided difference term depends on the function  $f(z)$ , and the appearance of the operator  $\hat{\mathbf{O}}$  is a setback to the original problem of approximating a function of an operator. The product term depends only on the interpolation points; therefore, instead of minimizing Equation 4.12, one can minimize the term

$$\bar{R}_{\min} = \text{Min} \left\| \prod_{j=0}^{N-1} \hat{\mathbf{Q}}_j \right\| \quad 4.13.$$

with respect to all interpolation points  $x_0, \dots, x_{N-1}$ . If the number of points is larger or equal to the number of eigenstates of  $\hat{\mathbf{O}}$ , the minimization is equivalent to diagonalizing  $\hat{\mathbf{O}}$  and choosing the interpolation points to be the eigenvalues. This equivalence to diagonalization, which should have been avoided, represents a drawback. Nevertheless, an important lesson can be learned from the formulation: choosing the interpolation points in regions where the eigenvalues of  $\hat{\mathbf{O}}$  reside will effectively improve the convergence of the polynomial approximation.

This finding is the unifying principle behind all the propagation methods. The various methods differ only in their strategy of minimizing the error in Equation 4.13. Two approaches to this problem have been developed depending on the method of calculating the norm in Equation 4.13. The uniform approach attempts to minimize the error with respect to all vectors in the Hilbert space of the problem (see below). The nonuniform approach tries to minimize the error with respect to a particular vector  $\psi$ , usually chosen to be the initial vector  $\psi(t = 0)$  (see below).

## UNIFORM APPROXIMATION APPROACH

As concluded in the previous section, a detailed knowledge of the positions of the eigenvalues of  $\hat{\mathbf{O}}$  completely determines the interpolation polynomial. Because this detailed description is usually prohibitively expensive, a strategy for choosing the interpolation points has to be developed based on only a partial knowledge of the location of the eigenvalues. The number of interpolation points, or the order of the polynomial, can be reduced to considerably less than the number of eigenvalues of  $\hat{\mathbf{O}}$ .

Consider the situation when the operator  $\hat{\mathbf{O}}$  is hermitian. As a result of this condition, all eigenvalues are located on the real axis, and the upper and lower bounds for the eigenvalues  $\lambda_n$  can be found for any pseudo-spectral representation of the elementary mapping step. The strategy is then to use this partial knowledge to construct a uniform approximation of the function  $f$  on the interval on the real axis defined by the upper and lower bounds of the eigenvalues. For the Hamiltonian operator, this will be the energy axis. The original problem of approximating the operation of a function of an operator has been transformed to the problem of finding the best uniform approximation of a scalar function  $f(z)$  on a closed interval  $\lambda_{\min} \leq z \leq \lambda_{\max}$ .

This is a classical problem in numerical analysis: finding a polynomial approximation so that the maximum error is minimum on this interval. The most general interpolation polynomial obeys the relation

$$f(z) = \mathcal{P}_N(z) + \frac{f^{N+1}[\xi(z)]}{(n+1)!} (z-x_0)(z-x_1)(z-x_2)\dots, \quad 5.1.$$

where  $x_n$  are sampling points and  $\xi$ , which is a function of  $z$ , is also included in the interval. To minimize the error regardless of its position in the interval, one can choose the sampling points  $x_n$  so that the product on the r.h.s. of Equation 5.1,

$$E(z) = \|(z-x_0)(z-x_1)(z-x_2)\dots\|, \quad 5.2.$$

is minimum for arbitrary  $z$  in the interval. This product is a monomic polynomial of degree  $N + 1$ . The minimax criteria can now be traced to a condition on Equation 5.2 that the maximum amplitude of  $E(z)$  in the interval is minimum. The Chebychev polynomial has uniform amplitude in the interval and therefore it obtains its maximum value  $N$  times with the value  $1/2^{N-1}$ . All other polynomials of the same degree become non-uniform and therefore have larger maximum amplitudes. As a result they are inferior to the Chebychev polynomial in reducing the error term  $E(z)$ .

The conclusion, therefore, is that minimizing the error is equivalent to choosing the sampling points as the zeros of the  $N + 1$  Chebychev polynomial. One can then proceed directly by using the Newtonian formulation of the interpolation polynomial.

### *Newtonian Polynomial Algorithm*

The analytic function  $f(z)$  is calculated at a set of support points  $\{z_k, f_k\}$ , where  $f_k = f(z_k)$ . The interpolation polynomial is used to approximate the function  $f(z)$ :

$$f(z) \approx \mathcal{P}_N(z) \equiv \sum_{n=0}^N a_n \mathcal{R}_n(z), \quad 5.3.$$

where  $\mathcal{R}_n(z)$  are the Newtonian polynomials of degree  $n$  defined by:

$$\mathcal{R}_n(z) \equiv \prod_{j=0}^{n-1} (z - z_j) \quad 5.4.$$

and  $\mathcal{R}_0(z) = 1$ . The coefficient  $a_n$  is the  $n$ th divided difference coefficient (35) defined as

$$a_0 = f_0, \quad a_1 = \frac{f_1 - f_0}{z_1 - z_0} \quad 5.5.$$

and, in general for  $n > 1$ ,

$$a_n = \frac{f_n - \mathcal{P}_{n-1}(z_n)}{\mathcal{R}_n(z_n)}. \quad 5.6.$$

Because the operator  $\hat{\mathbf{O}}$  is hermitian, the support points  $z_k$  are chosen on the real axis. For a Chebychev-based interpolation scheme, the points  $z_k$  are chosen as the zeros of the  $N + 1$  Chebychev polynomial,  $z_k = 2 \cos \theta_k$ , which defines points on the interval  $[-2, 2]$ . This choice of support interval ensures stability of the divided difference coefficients. The specific choice of interval has to be reflected in the spectrum of the operator which should go through a linear transformation to the  $[-2, 2]$  interval. This is done by

estimating the domain of eigenvalues of  $\hat{\mathbf{O}}$ ,  $\lambda_{\min}$ ,  $\lambda_{\max}$ . Then the linear transformed operator becomes

$$\hat{\mathbf{O}}_N = 4 \frac{\hat{\mathbf{O}} - \lambda_{\min}}{\lambda_{\max} - \lambda_{\min}} - 2, \quad 5.7.$$

and the operator  $\hat{\mathbf{O}}_N$  is used to generate the interpolation polynomials. The normalization of the operator is compensated by calculating the function  $f(z')$  in the divided difference coefficients at the points  $f[(\lambda_{\max} - \lambda_{\min})(z + 2)/4 + \lambda_{\min}]$ .

With this choice the recursion relation becomes

$$\phi_0 = \psi,$$

$$\phi_1 = (\hat{\mathbf{O}}_N - z_0)\phi_0,$$

and

$$\phi_{n+1} = (\hat{\mathbf{O}}_N - z_n)\phi_n. \quad 5.8.$$

The final result is obtained by accumulating the sum

$$\phi = \sum_{n=0}^{N-1} a_n \phi_n. \quad 5.9.$$

The sum is truncated when the residuum  $a_N \|\phi_N\|$  is smaller than a pre-specified tolerance. In order to stabilize high order polynomial expansions, the naive choice of sampling points,  $\theta_k = \pi(2k + 1)/(N + 1)$ , is unstable; therefore, a staggering strategy has to be employed. This leads to the choice

$$\theta_k = \text{Mod} \left\{ \frac{2\pi}{N} \left[ n + \frac{N}{n_{\text{stag}}} \text{Mod}(n, n_{\text{stag}}) \right], 2\pi \right\}, \quad 5.10.$$

where  $n = 0, 1, \dots, N - 1$ , and the parameter  $n_{\text{stag}}$  determines the amount of staggering. Maximum staggering is obtained by choosing  $n_{\text{stag}} = N/2$ . This point is quite amazing because Newton's interpolation polynomials are invariant to a permutation of points. On the other hand, numerically reordering the points completely changes the stability characteristics of the algorithm.

As an illustration, the evolution operator is considered, with  $\hat{\mathbf{O}} = \hat{\mathbf{H}}$  and  $f(z) = e^{-izt}$ . The number of terms in Equation 5.9 is determined by the volume of the time-energy phase space,  $N > \Delta Et/2\hbar$ , beyond which the evolution operator displays exponential convergence with respect to  $N$ . A simple monotonic ordering of points allowed a maximum order of  $N \approx 30$  before instabilities occurred. Simple two-point staggering increases

the maximum order to  $N \approx 150$ . A full staggering of points allows a stable propagation of polynomial orders larger than  $N = 100,000$ . This algorithm is a typical case of mathematically equivalent algorithms with different numerical implementations. There are two reasons for the instability in the Newtonian interpolations: first, the divided difference coefficients can become very large if the adjacent points are close, and second, the vectors  $\phi_n$  can overflow the numerical representation. The reordering and staggering are therefore crucial to the application of the method.

Changing the function  $f$  only requires recalculating the divided difference coefficients and resummation of the result. This change also means that intermediate results are obtainable without much extra numerical effort. Typical functions include  $f(z) = e^{-z\tau}$ . These will lead to a propagator that will relax an initial vector  $\psi$  to the ground state (Y Yamashita & R Kosloff, unpublished data), or  $f(z) = e^{-(z-\alpha)^2\tau}$ , which will lead to a propagator that relaxes to a stationary vector with the closest eigenvalue to  $\alpha$  (37) (see below). This derivation can be considered a pseudo-spectral scheme in the time-energy phase space, similar to the discrete variable representation (DVR) expansion method of Lill et al (32), which is used for position-momentum phase space.

### *Uniform Approximation for Non-Hermitian Operators*

Propagators generated from non-Hermitian operators are becoming an important part of the arsenal of methods in molecular dynamics. For example, absorbing potentials (38–44) are commonly used to absorb all outgoing flux with negligible back reflection. The absorbing potentials push the eigenvalues of the Hamiltonian into the complex negative plane. A closely related method to the use of complex absorbing potentials is the method of complex rotation (45, 45a,b), which also results in a complex valued Hamiltonian operator.

Extending the ideas of the previous section, the first step is to identify the region in the complex plane where the eigenvalues of the operator  $\hat{O}$  can be located. The most simple setup is to assume that all eigenvalues are located within a circle of radius  $\rho$  in the complex plane. A uniform polynomial approximation of the region within the circle can be obtained by placing the interpolation points on the circumference of the disc. For the sake of symmetry, these points have to be uniformly distributed on the circle

$$z_n = Z + \rho e^{-2\pi i((N/2)-1)n/N}, \quad 5.11.$$

where  $Z$  is the center of the circle. Except for the different choice of sampling points, the algorithm is identical to the Hermitian case of Equations 5.3–5.9.

In many cases, the circle used to confine the eigenvalues of  $\hat{\mathbf{O}}$  leaves a large empty area with no eigenvalues. An extreme example is the hermitian operator considered above where the eigenvalues are located on the real axis. A solution to this problem is to confine the eigenvalues of  $\hat{\mathbf{O}}$  by a polygon. The interpolation points are located on this polygon and are found by identifying a conformal mapping from the polygon to the disc (46). The sampling points are found on the circumference of the disc by symmetry considerations, i.e. Equation 5.11. Then, the inverse transform determines the position of the points on the polygon. Once the points  $z_n$  are determined, the algorithm proceeds as described above.

A typical example of the use of the nonuniform propagating method is for the Liouville von Neumann equation (25),

$$\frac{\partial \hat{\rho}}{\partial t} = \mathcal{L} \hat{\rho}, \quad 5.12.$$

where  $\hat{\rho}$  is the density operator and  $\mathcal{L}$  is the Liouville super-operator. For an open dissipative system,  $\mathcal{L}$  has complex eigenvalues.  $\mathcal{L}$  can be decomposed into  $\mathcal{L} = \mathcal{L}_H + \mathcal{L}_D$  where  $\mathcal{L}_H = -i[\hat{\mathbf{H}}, \ ]$ , which is a super-operator with purely imaginary eigenvalues.  $\mathcal{L}_D$  represents the dissipative part representing the approach to thermal equilibrium (47). The solution to the Liouville von Neumann equation,

$$\hat{\rho}_t = e^{\mathcal{L}t} \hat{\rho}_0, \quad 5.13.$$

suggests the function  $f(z) = e^{zt}$ . The initial vector  $|\psi\rangle$  becomes the density operator  $\rho_0$ . The eigenvalue range on the imaginary axis is determined by  $\mathcal{L}_H: 2\Delta E$  while the range on the real axis is always negative represented by  $\mathcal{L}_D$ . The eigenvalue representing equilibrium is located on the real axis. Applications of the method can be found in Ref. 48.

A more involved application is to solve the reactive scattering problem with a modified Lippmann-Schwinger equation (49) with absorbing boundary conditions (50)

$$|\Psi^{ABC}(E)\rangle = \hat{\mathbf{G}}^{ABC}(E) i\hat{\varepsilon}(\hat{\mathbf{q}}) |\Phi(E)\rangle, \quad 5.14.$$

where  $\hat{\varepsilon}(\hat{\mathbf{q}})$  is a coordinate dependent operator, and

$$\hat{\mathbf{G}}^{ABC} = (E + i\hat{\varepsilon} - \hat{\mathbf{H}})^{-1}. \quad 5.15.$$

The Fourier integral transforms the equation to the form

$$\hat{\mathbf{G}}(E) = (i\hbar)^{-1} \int_0^\infty dt e^{i(E + i\hat{\varepsilon} - H)t/\hbar}. \quad 5.16.$$

The long time exponential is represented as a product of short time exponentials:

$$G(E) = (i\hbar)^{-1} \sum_{n=0}^{\infty} [e^{iE\Delta t/\hbar} e^{-i(\hat{H}-i\epsilon)\Delta t/\hbar}]^n \int_0^{\Delta t} dt e^{iEt/\hbar} e^{-i(\hat{H}-i\epsilon)t/\hbar}. \quad 5.17.$$

This equation was the starting point for Auerbach & Leforestier (7) to use a polynomial expansion,

$$\hat{G}(E) \approx (i\hbar)^{-1} \sum_{n=0}^N \left[ \sum_{k=0}^K c_k(E, \Delta t) \mathcal{P}_k(\hat{H} - i\epsilon) \right]^n \sum_{k'=0}^K b_{k'}(E, \Delta t) \mathcal{P}_{k'}(\hat{H} - i\epsilon), \quad 5.18.$$

where  $c_k(E, t) = e^{iEt/\hbar} a_k(t)$  and  $b_k = \int_0^t d\tau e^{iE\tau/\hbar} a_k(\tau)$  and  $\mathcal{P}_k$  are the recursive polynomials of Equation 5.4. The coefficients  $a_k$  were determined by using Equations 4.8 and 4.9 with  $f = e^{izt}$ . The sampling points, which are located on a half circle in the complex plane (see Figure 1), were

$$z_k = \begin{cases} \cos \theta_k, & \theta_k \in [0, \pi] \\ e^{i\theta_k}, & \theta_k \in [\pi, 2\pi] \end{cases}. \quad 5.19.$$

The method has been applied to the 3-D reactive scattering of  $D + H_2$  (8).

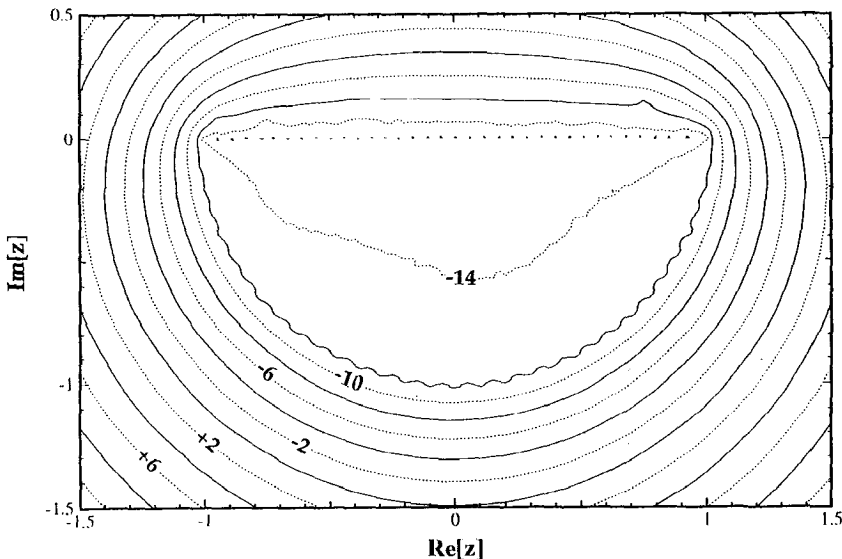


Figure 1 Contour map of interpolation accuracy for the function  $e^{izt}$  for  $t = 20$ , using the Newtonian interpolation function with the 64 points defined by Equation 5.19.

## NONUNIFORM APPROXIMATION

The distinction between uniform and nonuniform approximation is in the strategy by which the interpolation error is minimized in Equations 4.12 and 4.13. In the nonuniform approximation, the initial vector  $\psi(0)$  plays a major role in minimizing the error. The Krylov vectors  $\phi_n = \hat{\mathbf{O}}^n \psi(0)$  can be considered the primitive base for the mapping of the interpolation polynomial. As will become clear in this section, many closely related Krylov space algorithms are based on this idea.

As was discussed in an earlier section, choosing the eigenvalues as interpolation points is an exact representation. This naturally leads to the idea that the use of approximate eigenvalues in a truncated space will create an effective algorithm. One such method is to use the Krylov vectors  $\phi_n$  up to order  $N$  as the base for a truncated representation of  $\hat{\mathbf{O}}$  leading to the generalized eigenvalue equation

$$\tilde{\mathbf{O}}\tilde{x} = \lambda\tilde{\mathbf{S}}\tilde{x}, \quad 6.1.$$

where  $(\tilde{\mathbf{O}})_{nm} = \langle \phi_n | \hat{\mathbf{O}} | \phi_m \rangle = \langle \phi_n | \phi_{m+1} \rangle$ , and  $(\tilde{\mathbf{S}})_{nm} = \langle \phi_n | \phi_m \rangle$  is the overlap matrix. Once the eigenvalues  $\lambda_k$  are calculated, they are used as interpolation points, and the algorithm proceeds as before. Because the order of the truncated space is much smaller than the order of the representation of  $\hat{\mathbf{O}}$ , the numerical effort in solving Equation 6.1 is negligible.

Another approach is to minimize the norm of the error vector  $\langle \chi | \chi \rangle$  defined by

$$\chi = R(\hat{\mathbf{O}})\psi = f[x_0, x_1, \dots, x_N, \hat{\mathbf{O}}](\hat{\mathbf{O}} - x_N \hat{\mathbf{I}})(\hat{\mathbf{O}} - x_{N-1} \hat{\mathbf{I}}) \dots (\hat{\mathbf{O}} - x_0 \hat{\mathbf{I}}), \quad 6.2.$$

where the minimization is with respect to the sampling points  $x_0, x_1, \dots, x_N$ . For the general case, evaluating the mapping of the operator  $f[x_0, x_1, \dots, x_N, \hat{\mathbf{O}}]$  is extremely difficult because the divided difference coefficients are rational fractions and not polynomials. To overcome this difficulty, one can minimize only the norm of the vector produced by the RHS of Equation 6.2:

$$\bar{\chi} = \bar{R}(z)\psi = (\hat{\mathbf{O}} - x_N \hat{\mathbf{I}})(\hat{\mathbf{O}} - x_{N-1} \hat{\mathbf{I}}) \dots (\hat{\mathbf{O}} - x_0 \hat{\mathbf{I}})\psi, \quad 6.3.$$

with respect to the  $N$  sampling points. To simplify the minimization problem, Equation 6.3 can be rewritten as a power expansion:

$$\bar{\chi} = \bar{R}(z)\psi = \sum_{k=0}^{N+1} d_k \hat{\mathbf{O}}^k \psi = \sum_{k=0}^{N+1} d_k \phi_k, \quad 6.4.$$

where the minimization procedure is now transformed to the  $d_k$  coefficients.

Notice that  $d_{N+1} = 1$  because the polynomial in Equation 6.3 is monomic. The norm of  $\bar{\chi}$  with respect to the  $d_k$  coefficients is a quadratic expression:

$$\langle \bar{\chi} | \bar{\chi} \rangle = \sum_{i=0}^N \sum_{j=0}^N d_i d_j \langle \phi_i | \phi_j \rangle + \text{const.} \quad 6.5.$$

The minimalization of the Residuuum 6.5 leads to the linear expression for the  $d_i$  vector,

$$\tilde{\mathbf{S}} \mathbf{d} = \mathbf{b}, \quad 6.6.$$

where the overlap matrix  $\tilde{\mathbf{S}}$  is defined as

$$S_{ij} = \langle \phi_i | \phi_j \rangle, \quad 6.7.$$

and the  $\mathbf{b}$  vector becomes

$$b_i = -\langle \phi_i | \phi_{N+1} \rangle \quad 6.8.$$

because the polynomial (Equation 6.3) is monomic,  $d_{N+1} = 1$ . Once the coefficients  $d_k$  are known, solving for the roots of  $\bar{R}(z)$  gives the desired optimal interpolation points. A twist on this procedure is obtained if the primitive Krylov base is orthonormalized by a Gram-Schmidt procedure, e.g.  $\xi_1 = \phi_1$  and  $\xi_2 = \phi_2 - \langle \phi_2 | \xi_1 \rangle \xi_1$ . The result is a diagonal overlap matrix  $\tilde{\mathbf{S}}$ . Then, minimizing the residuum in this functional base  $\bar{R}(z)\psi = \sum_{j=0}^{N+1} e_j \xi_j$  leads to  $e_k = 0$  for  $k \leq N+1$  and  $e_{N+1} = 1$ . The interpretation of this is that the minimum residuum vector is orthogonal to all other vectors in the Krylov space. As a consequence, the use of an orthonormal Krylov subspace automatically minimizes the interpolation error. This means that an alternative procedure for obtaining the interpolation points is to find the eigenvalues of the Hamiltonian in the truncated orthogonal Krylov space. This can be done simultaneously during the creation of the Krylov space by using the procedure

$$\xi_0 = \psi \quad 6.9.$$

and

$$\hat{\mathbf{O}} \xi_0 = \alpha_0 \xi_0 + \beta_0 \xi_1, \quad 6.10.$$

and generally

$$\hat{\mathbf{O}} \xi_n = \beta_{n-1} \xi_{n-1} + \alpha_n \xi_n + \beta_n \xi_{n+1}, \quad 6.11.$$

where  $\alpha_n = \langle \xi_n | \hat{\mathbf{O}} | \xi_n \rangle$  and  $\beta_{n-1} = \langle \xi_{n-1} | \hat{\mathbf{O}} | \xi_n \rangle$ . This procedure, which is due to Lanczos (16), leads to a tridiagonal truncated representation of the operator  $\hat{\mathbf{O}}$ . The eigenvalues of this truncated space can now be used as

interpolation points in Equation 5.9. The solution of the characteristic equation and the location of the zeros of the polynomial  $\bar{K}(z)$  for the minimum residuum case coincide. The three methods are mathematically equivalent but are algorithmically different. They suffer from the drawback that the recursion is done twice, once for the Krylov space and once for the Newtonian interpolation. But considering that the interpolation points do not have to be changed for every time-step, the additional work is not large. The first algorithm (Equation 6.1) is the most stable numerically.

Instead of minimizing the residuum vector  $\bar{\chi}$  in Equation 6.2, a slight alteration leads to minimizing  $\tilde{\chi}$  which is the optimal choice for the function  $f(z) = 1/z$ :

$$\tilde{\chi} = \frac{1}{x_N}(\hat{\mathbf{O}} - x_N \hat{\mathbf{I}}) \frac{1}{x_{N-1}}(\hat{\mathbf{O}} - x_{N-1} \hat{\mathbf{I}}) \dots \frac{1}{x_0}(\hat{\mathbf{O}} - x_0 \hat{\mathbf{I}})\psi. \quad 6.12.$$

The algorithm that minimizes  $\tilde{\chi}$  is slightly better than the one that minimizes  $\bar{\chi}$  (22).

An alternative approach that saves the need to calculate the Newtonian recursion is to use the Krylov vectors directly:

$$f(\hat{\mathbf{O}})\psi \approx \phi = \sum_{n=0}^{N-1} c_n \phi_n, \quad 6.13.$$

where the expansion coefficients are those described in Ref. (22). By using the orthogonal Krylov vectors  $\zeta_n$  (20, 21), the function becomes

$$f(\hat{\mathbf{O}})\psi \approx \phi = \sum_{n=0}^{N-1} e_n \zeta_n, \quad 6.14.$$

and the expansion coefficients become

$$e_n = \{\mathbf{Z}^\dagger \mathbf{D}[f(\lambda_m)]\mathbf{Z}\}_{1n}, \quad 6.15.$$

where  $\mathbf{Z}$  are the matrices that diagonalize  $\hat{\mathbf{O}}$  in the Krylov subspace of  $\psi$  and  $\lambda$  are the eigenvalues in this subspace. The common exponential function in the propagator has been replaced with sine and cosine functions, thereby splitting the propagation into real and imaginary components (51).

The Krylov-type expansion can be applied with non-Hermitian operators. One method is to find approximate eigenvalues in a truncated Krylov space and then use the Newtonian interpolation method (A Bartana & R Kosloff, unpublished data). As an alternative, the short iterative Arnoldi method has been developed by Pollard & Friesner (53). It explicitly addresses the fact that  $\hat{\mathbf{O}}$  is non-Hermitian and therefore has left and right eigenfunctions as the recursion is carried out.

To summarize, there has been a proliferation of Krylov space-based methods. In practice, the optimal order  $N$  of these polynomial expansions is practically  $N \approx 5-12$ , which is the reason for the generic term SIL, for a short iterative Lanczos method. The maximum order is limited to about  $N = 30$  because of numerical instabilities. The source of this instability is the orthogonalization step. This means that the common use of these algorithms is quite different from the uniform approximations; they are usually used for short time propagators.

## SPECTRAL REPRESENTATION OF THE UNIFORM APPROXIMATION

Throughout this review, the time-energy phase space has been treated by a global functional approach. This means that an algorithm for the function of an operator can be based on a functional expansion. The functional expansion approach seeded the original development of the Chebychev method (1). Because the basic mapping allows only polynomial expansions, an algorithm must be based on one of the known orthogonal polynomials. The Chebychev polynomials are the only ones studied in detail, although other polynomial expansions have also been tried out (10). Compared to representation in the position-momentum phase space, the functional expansion is considered a spectral approximation, and the point representation is a pseudo-spectral method. Later in this section, we will demonstrate that the two approaches are equivalent.

### *Basic Chebychev Expansion Algorithm*

The following is a description of the algorithm. The usual definition of the Chebychev polynomials is on the interval  $-1$  to  $1$ ; therefore, a linear transformation is applied to the argument  $z$ :

$$z' = 2 \frac{z - \lambda_{\min}}{\lambda_{\max} - \lambda_{\min}} - 1. \quad 7.1.$$

An expansion by Chebychev polynomials explicitly becomes

$$f(z) \approx \sum_{n=0}^N b_n T_n(z') \quad 7.2.$$

for the function  $f(z)$ , where  $T_n$  is the Chebychev polynomial of degree  $n$ , and  $b_n$  are expansion coefficients defined by

$$b_n = \frac{2 - \delta_n}{\pi} \int_{-1}^1 \frac{f(z') T_n(z')}{\sqrt{1 - z'^2}} dz'. \quad 7.3.$$

Returning now to the problem of approximating  $\phi = f(\hat{\mathbf{O}})\psi$ , the approximation is obtained by replacing the argument  $z'$  with the operator  $\hat{\mathbf{O}}$ . This is done in the following steps:

1. Calculating the expansion coefficients  $b_n$  using Equation 7.3.
2. Applying a linear transformation to the operator  $\hat{\mathbf{O}}$ :

$$\hat{\mathbf{O}}' = 2 \frac{\hat{\mathbf{O}} - \lambda_{\min} \hat{\mathbf{I}}}{\lambda_{\max} - \lambda_{\min}} - \hat{\mathbf{I}}. \quad 7.4.$$

3. Using the recursion relation of the Chebychev polynomials to calculate  $\phi_n$ , where

$$\begin{aligned} \phi_0 &= \psi, \\ \phi_1 &= \hat{\mathbf{O}}' \psi, \end{aligned} \quad 7.5.$$

and

$$\phi_{n+1} = 2\hat{\mathbf{O}}' \phi_n - \phi_{n-1}. \quad 7.6.$$

Again, the calculation of the recursion is based on the ability to perform the discrete mapping caused by the operator  $\hat{\mathbf{O}}$ . Two basic operations are used for the recursion: multiplication (mapping) by an operator on a vector and an addition of another vector.

4. Accumulating the result while calculating the recursion relation by multiplying  $b_n$  by  $\phi_n$  and adding to the previous result:

$$\phi = \sum_{n=0}^N b_n \phi_n. \quad 7.7.$$

5. Truncating the calculation when the desired accuracy has been obtained.

It should be noted that the Chebychev recursion relation, which consumes most of the numerical effort, is independent of the function  $f$  to be approximated. This means that many different functions  $f$  can be approximated simultaneously by repeating steps 2, 4, and 5. The uniform nature of the approximation means the error is independent of the choice of the initial vector  $\psi$ .

### *Generic Examples of the Chebychev Expansion Method*

Considering the time-dependent Schrödinger equation,  $i\hbar(\partial\psi/\partial t) = \hat{\mathbf{H}}\psi$ , and its formal solution  $\psi(t) = e^{-(i/\hbar)\hat{\mathbf{H}}t}\psi(0)$ , the function  $f(z)$  to be approximated is  $e^{-iz}$ . Following the steps of the algorithm, the range of energy  $\Delta E = E_{\max} - E_{\min}$  represented by  $\hat{\mathbf{H}}$  is estimated. The shift operation causes

a phase shift in the final wavefunction that can be readjusted by multiplying  $\phi$  by the phase factor

$$\Phi(t) = e^{(i\hbar)(\Delta E/2 + E_{\min})t}, \quad 7.8.$$

The expansion coefficients  $b_n$  are calculated from Equation 7.3 to obtain

$$b_0 = J_0\left(\frac{\Delta E \cdot t}{2\hbar}\right)\Phi \quad 7.9.$$

and

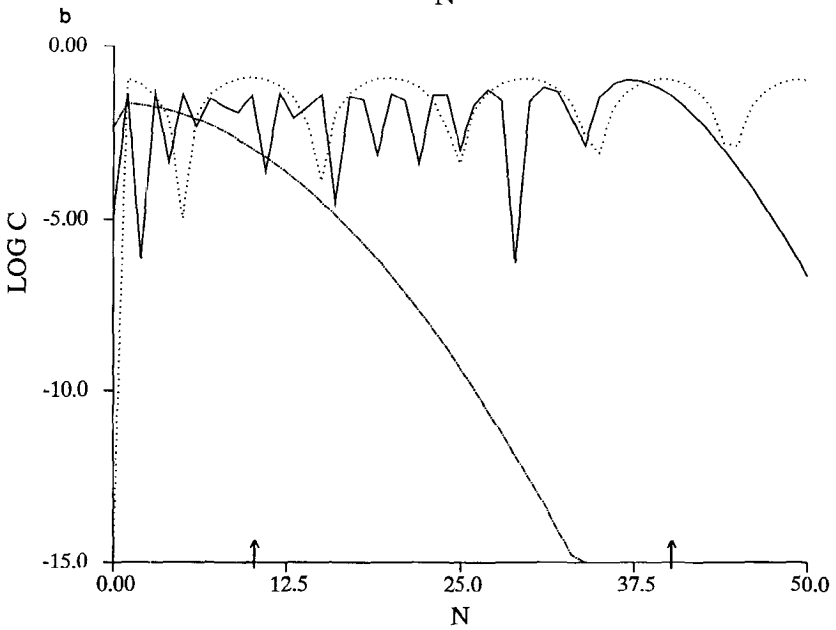
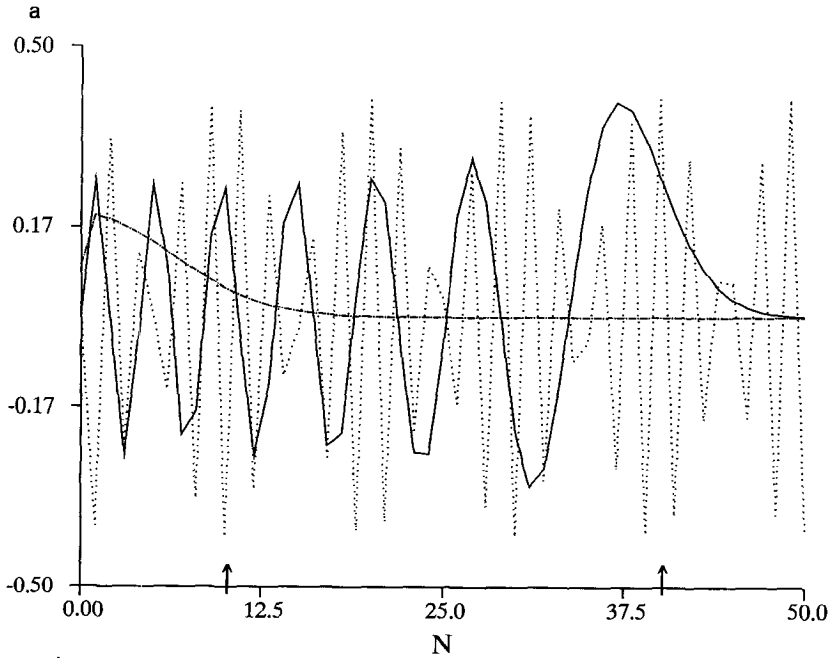
$$b_n = 2i^n J_n\left(\frac{\Delta E \cdot t}{2\hbar}\right)\Phi \quad n \neq 0, \quad 7.10.$$

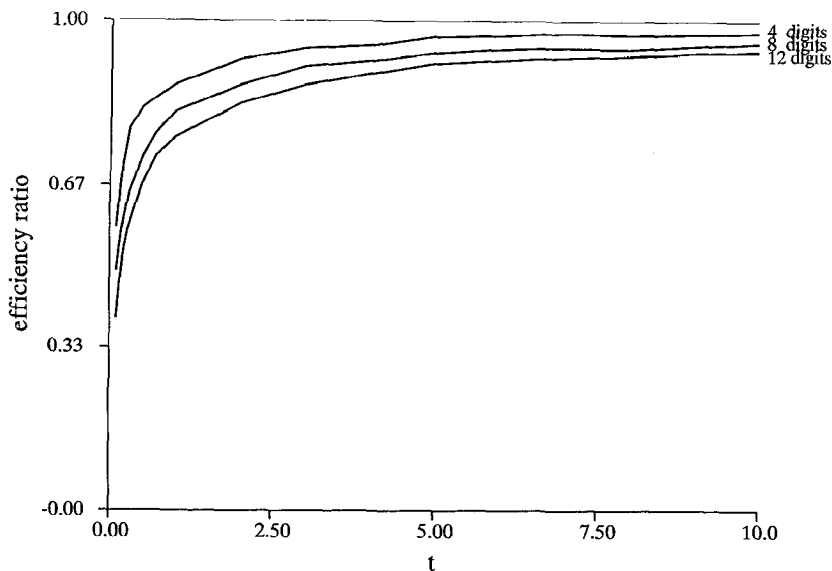
where  $J_n$  are Bessel functions. The argument of the Bessel function,  $\Delta E \cdot t/2\hbar$ , is related to the volume of the time-energy phase space that is contained in the problem. The number of terms  $N$  needed to converge the expansion is determined by this volume. This is because of an asymptotic property of the Bessel function: When the order  $n$  becomes larger than the argument, the Bessel function,  $J_n$ , decreases exponentially fast (see Figure 2). The Chebychev vectors  $\phi_n$  are functions of the normalized Hamiltonian and the initial wavefunction  $\psi$ . Therefore intermediate results can be obtained by calculating another set of coefficients  $b_n$  and repeating the resummation step. Figure 2 shows the relation between the number of terms needed to achieve convergence and the propagated time interval. The linear relationship is clearly seen going up to very high orders of the polynomial. To check the limit of the expansion, a propagation for a time interval of 400 cycles of an oscillator has been tried. The resulting polynomial expansion was of the order of  $N = 120,000$ . The norm energy and overlap with the initial state all achieved an accuracy of 14 digits. This behavior is typical of the uniform convergence of the method where all error indications are of the same order of magnitude.

Figure 3 shows the efficiency ratio defined as the time-energy phase space volume divided by the number of terms in the expansion needed to

---

*Figure 2* Amplitude of the expansion coefficients of a Chebychev polynomial expansion for the functions  $e^{-iz}$  (solid line),  $e^{-z}$  (broken line), and  $1/z - \omega$  (dashed line) as a function of the order  $n$ .  $\Delta Et/2\hbar$  is chosen to be 40, and the point is indicated by the right arrow. Beyond this point, the expansion coefficients of the real-time propagator decay exponentially. The point  $(\Delta Et/2\hbar)^{1/2}$  is indicated by the left arrow showing the point where the imaginary time propagation decays exponentially. Figure 2*b* shows the same picture where the coefficients are displayed in a logarithmic scale. The exponential convergence of the propagators is clearly shown in comparison to the absence of convergence of the coefficients of the Resolvent.





*Figure 3* The efficiency ratio of the propagator defined as  $\Delta Et/2N\hbar$ , where  $N$  is the number of expansion terms plotted as a function of time. The three lines correspond to 12 digits of accuracy, 8 digits of accuracy, and 4 digits of accuracy. As time progresses the three lines reach their asymptotic value of 1. For short time, the efficiency deteriorates reaching 50% for a time of 0.1 periods (40 terms).

obtain convergence:  $\eta = (\Delta E \cdot t/2\hbar)/N$  as a function of time. The efficiency approaches one for long time propagations. For short time intervals, the efficiency decreases, which means that the overhead of points needed to obtain a prespecified accuracy increases. This is the reason that the Chebychev propagation method is recommended for very long propagation times. As the error is uniformly distributed and can be reduced to the precision determined by the computer, the Chebychev scheme is a fast, accurate, and stable method for propagating the time-dependent Schrödinger equation. The method is not unitary by definition and because of the uniform nature of the error distribution deviation from unitarity, which becomes extremely small, can be used as a check of accuracy. A vast number of applications in molecular dynamics stress this point (21). A useful twist in the Chebychev-based propagator is to replace the exponential function  $e^{izt}$  with  $\cos zt$  and  $\sin zt$  (51). This method allows a separation of the propagation into the real and imaginary parts of the wavefunction, for example,

$$\cos(\hat{H}_N t)\psi_R(t) = \sum_{n=0}^{N/2} (-1)^n b_{2n} \phi_{2n/R}, \quad 7.11.$$

where  $\phi_{n/R}$  are obtained by running the Chebychev recurrence (Equation 7.6) only on the real part of  $\psi(0)$ . If the initial wavefunction is real, this method can save half the numerical effort by changing from complex to a real representation of the wavefunction.

For comparison, the evolution operator can also be obtained by a Legendre expansion (10). The expansion coefficients become

$$b_n = (2n+1)(-1)^n \sqrt{\frac{\pi\hbar}{2\Delta E t}} J_{n+1/2}(\Delta E t/\hbar), \quad 7.12.$$

with the property that when  $N+1/2 > \Delta E t/\hbar$ , the coefficients also decay exponentially. The vectors  $\phi_n$  can be calculated by the Legendre recursion relation,  $\phi_0 = \Psi$ ,  $\psi_1 = \hat{\mathbf{O}}\psi$  and  $\phi_{n+1} = 2\hat{\mathbf{O}}\phi_n - \phi_{n-1} - [\hat{\mathbf{O}}\phi_n - \phi_{n-1}]/(n+1)$ , and the result is accumulated as in Equation 7.7.

### *Eigenvalues and Eigenfunctions by Propagation*

A small change in the function  $f$  leads to an effective method for obtaining the ground state and several low lying excited states. Considering the propagation of a vector  $\psi$ :

$$\phi = e^{-\hat{\mathbf{H}}\tau}\psi, \quad 7.13.$$

when  $\tau \rightarrow \infty$ ,  $\phi$  approaches the ground state exponentially fast. A proof for this is obtained by expanding  $\psi$  in the eigenstates of  $\hat{\mathbf{H}}$ ,

$$e^{-\hat{\mathbf{H}}\tau}\psi = \sum_n e^{-E_n\tau} u_n, \quad 7.14.$$

which converges to the ground state at a rate of  $e^{-(E_1-E_0)\tau}$ . By choosing  $f(z) = e^{-z}$ , the previous algorithm can be modified by performing analytic continuation of the expansion coefficients to obtain

$$b_0 = I_0(\alpha) \cdot N \quad 7.15.$$

and

$$b_n = 2I_n(\alpha) \cdot N, \quad 7.16.$$

where  $\alpha = \Delta E \cdot \tau/2$  and  $I_n$  are modified Bessel functions, and  $N = e^{+(1/2\Delta E + E_{\min})\tau}$ . These expansion coefficients converge exponentially because the modified Bessel functions  $I_n$  decay exponentially when  $n > (\Delta E \cdot \tau/2)^{1/2}$ . By comparison, this convergence is faster than the coefficients  $b_n$  of Equation 7.10. It should be noticed that Equation 7.13 becomes the solution to the diffusion or heat equation when the Hamiltonian operator is replaced by the appropriate diffusion operator (54). This means that the same algorithm can be used to solve these equations.

The scaling of the numerical effort as the square root of time has physical significance in the diffusion equation, for which the higher eigenvalues lose their significance as time progresses until at equilibrium only the lowest eigenvalue is of importance. Consider, for example, obtaining the ground state of the Harmonic oscillator from a coherent initial state, which means that the projections on the ground state and first excited state are approximately equal. The convergence is exponential with the relaxation constant approximately as predicted from Equation 7.14, for an harmonic oscillator of frequency 1. Considering that the numerical effort scales as  $(\tau)^{1/2}$  the numerical convergence is faster than exponential. The method can be modified to obtain excited eigenvalues and eigenfunctions by projecting out the lower eigenfunctions from the vector  $\phi_n = \hat{\mathbf{O}}\phi_{n-1}$ .

If one is interested in obtaining highly excited states a strategy aiming directly at them is advantageous. Neuhauser (12) has developed such a strategy based on a two-step approach. First with an initial guess containing the target energy range, a number of wavepackets are filtered out. This is done by propagating with a filter function:

$$f(z) = \int_{-\Delta t}^{\Delta t} dt e^{i(z-E)t} g(t), \quad 7.17.$$

where  $g(t)$  is a filter function chosen as a sum of decaying exponentials. This propagation filters out a wavefunction that has an energy in the range  $E$ . The procedure is repeated to generate wavefunctions covering an energy range  $\Delta E$ . After this step is completed, the generated wavefunctions are used as a base to represent a truncated Hilbert space spanning the energy range. Then the eigenfunctions are obtained by diagonalizing the Hamiltonian operator in this truncated basis (Equation 6.1). Variations of the above method come to mind such as using the filtered wavefunction as an initial vector for a Krylov space expansion.

Adiabatic switching is a different route to obtain eigenfunctions. One would start from a reference operator  $\hat{\mathbf{H}}_0$  whose eigenfunctions are known and then adiabatically turn on a perturbation  $\hat{\mathbf{V}}$  leading to the final operator,  $\hat{\mathbf{H}} = \hat{\mathbf{H}}_0 + \lambda(t_{\text{final}})\hat{\mathbf{V}}$ . By propagating the initial eigenfunction with a time-dependent operator,  $\hat{\mathbf{H}}(t) = \hat{\mathbf{H}}_0 + \lambda(t)\hat{\mathbf{V}}$ , the final eigenfunction should result, provided  $\lambda(t)$  is a slowly varying function of time. The method requires a high quality propagator for time-dependent operators (see below). A study by Kohen & Tannor (55) has shown disappointing results because the convergence was very slow. The problem is an intrinsic property of the adiabatic theorem because the use of an extremely high-quality propagator did not improve the results. A similar method has been applied to obtain resonances of an atom in a high electromagnetic field

when the power was turned on adiabatically. The degeneracy of the resonances with the continuum was eliminated by the complex rotation method (56). A method to obtain eigenvalues through the spectral density has recently been developed by Zhu et al (57). This development is closely related to the next subsection.

### Resolvent Function

Another important example is the Resolvent operation,

$$\hat{\mathbf{G}}(E) = \frac{i}{2\pi} \frac{1}{E - \hat{\mathbf{H}}}. \quad 7.18.$$

Applications include scattering or the calculation of Raman or absorption spectra. The expansion coefficients can be obtained either directly or by a Fourier transform of the expansion coefficients of Equation 7.10 by using the identity of the Fourier transform pair:

$$i^n J_n(x) \Leftrightarrow \begin{cases} \frac{2}{\pi} \frac{T_n(z)}{(1-z^2)^{1/2}} & \text{for } |z| < 1 \\ 0 & \text{for } |z| > 1 \end{cases}. \quad 7.19.$$

The coefficients become

$$b_0 = \frac{2}{\pi} \frac{1}{(1-\alpha^2)^{1/2}} \quad b_n = \frac{4T_n(\alpha)}{\pi(1-\alpha^2)^{1/2}}, \quad 7.20.$$

where  $\alpha = E - \bar{E}/\Delta E$ , with  $\bar{E} = \frac{1}{2}(E_{\max} + E_{\min})$ . The coefficients  $b_n$  do not converge when  $n \rightarrow \infty$  and, therefore, the sum in Equation 7.7 has to converge due to the properties of  $\phi_n$ . An alternative expression to Equation 7.20 has been obtained by Hoang et al (9, 9a), which leads to

$$b_n(E) = (2 - \delta_{n0}) \frac{[(E - \bar{E}) - i\sqrt{(\Delta E)^2 - (E - \bar{E})^2}]^n}{2\pi(\Delta E)^n \sqrt{(\Delta E)^2 - (E - \bar{E})^2}}. \quad 7.21.$$

As an illustration, the power absorbed from a continuous wave (CW) laser becomes (61)

$$\mathcal{P}(\omega) = \omega B \int_{-\infty}^{\infty} d\tau e^{i(\omega + \omega_0)\tau} \langle \theta_0 | e^{-(i/\hbar)\hat{\mathbf{H}}_{\text{ex}}\tau} | \theta_0 \rangle, \quad 7.22.$$

where  $\theta_0 = \hat{\mu}\psi_g(0)$ ,  $\hat{\mu}$  is the transition dipole operator,  $\hat{\mathbf{H}}_{\text{ex}}$  is the excited state Hamiltonian, and  $B = |E_0|^2/4\hbar$ . The absorption cross section becomes proportional to

$$\sigma(\omega) \propto \left\langle \theta(0) \left| \frac{1}{\hat{\mathbf{H}}_{\text{ex}} - \omega} \right| \theta(0) \right\rangle. \quad 7.23.$$

Applying Equations 7.20 and 7.23, the spectrum becomes

$$\sigma(\omega) \propto \sum_{n=0}^N b_n(\omega/\Delta E) \langle \psi(0) | \phi_n \rangle, \quad 7.24.$$

where  $\phi_n$  are the Chebychev vectors obtained from Equation 7.6 with the excited state Hamiltonian and initial wavefunction  $\psi(0)$ . Figure 2 compares the expansion coefficients of the three examples. Equation 7.23 converges, provided that the overlap of the Chebychev vectors with  $\theta(0)$  decays fast enough as is typical of a photodissociation spectrum. Comparing the polynomial expansions for the evolution operator and the Resolvent operator, the convergence of the evolution operator is generally found to be faster. The mathematical reason is the singularity in the Resolvent function compared to the analytic properties of the function  $f(z) = e^{iz}$ .

### Correlation Functions

The one time correlation function  $\langle \psi(0) | \phi(t) \rangle$  and its Fourier transform  $\int dt e^{-i\omega t} \langle \psi(0) | \phi(t) \rangle$  can be calculated by the standard Chebychev methods (Equation 7.24) because only one wavefunction has to be propagated (13, 14). A two-time correlation function constructed from a product of two distinct wave packets is more difficult. This type of integral is extremely useful for many applications such as flux calculations in scattering (58) and reactive scattering problems. The integral of interest is given by the following equation:

$$I(t, R) = \int_0^t \chi^*(t - \tau, R) \Psi(\tau, R) d\tau, \quad 7.25.$$

where both  $\Psi(t)$  and  $\chi(t)$  are time-dependent wave functions:

$$\Psi(\tau) = e^{-(i/\hbar)\hat{\mathbf{H}}\tau} \Psi(0)$$

and

$$\chi(\tau) = e^{-(i/\hbar)\hat{\mathbf{H}}\tau} \chi(0). \quad 7.26.$$

Equation 7.25 then becomes

$$I(t, R) = \int_0^t [e^{-(i/\hbar)\hat{\mathbf{H}}(t-\tau)} \chi(0, R)]^* e^{-(i/\hbar)\hat{\mathbf{H}}\tau} \Psi(0, R) d\tau. \quad 7.27.$$

The two wavepackets using the truncated Chebychev expansion of the evolution operator (39) become

$$\Psi(\tau, R) = \Phi(\tau) \sum_{n=0}^N a_n \left( \frac{\Delta E \tau}{2\hbar} \right) \phi_n(R)$$

and

$$\chi(t-\tau, R) = \Phi(t-\tau) \sum_n^N a_n \left( \frac{\Delta E(t-\tau)}{2\hbar} \right) \theta_n(R). \quad 7.28.$$

The symbols  $\phi_n(R)$  and  $\theta_n(R)$  denote the functions obtained from the Chebychev recursion initiated by  $\Psi$  and  $\chi$ . With this expansion, the time integral (Equation 7.27) becomes

$$I(t, R) = \Phi(t) \sum_{n,m} \left[ \int_0^t B_m \left( \frac{\Delta E(t-\tau)}{2\hbar} \right) B_n \left( \frac{\Delta E \tau}{2\hbar} \right) d\tau \right] \theta_m(R)^* \phi_n(R). \quad 7.29.$$

A property of the Bessel functions enables replacement of the correlation integral by an infinite series (35):

$$\int_0^x J_n(x-y) J_m(y) dy = 2 \sum_{k=0}^{\infty} (-1)^k J_{n+m+2k+1}(x). \quad 7.30.$$

Rearranging terms and using Equation 7.30, enables the time-integral (Equation 7.25) to be represented by the following expression:

$$I(t, R) = \sum_{n,m} A_{n+m}(t) \theta_m(R)^* \phi_n(R). \quad 7.31.$$

The coefficients  $A_{n+m}(t)$  are defined as

$$A_{n+m}(t) = (2 - \delta_{n0})(2 - \delta_{m0}) \frac{4\hbar}{\Delta E} \Phi(t) \left[ \sum_{k=0}^{\infty} (-1)^k J_{n+m+2k+1} \left( \frac{\Delta E}{2\hbar} t \right) \right]. \quad 7.32.$$

For a given value of  $t$ , the Bessel series  $\{J_n(\Delta E \cdot t/2\hbar)\}_{n>\Delta E t/2\hbar}^{\infty}$  exhibits exponentially rapid decay to zero as  $n$  is increased. Therefore, both sums in Equations 7.31 and 7.32 display exceedingly stable numerical convergence. The correlation function  $\langle \Psi(t) | \chi(t) \rangle$  can be obtained in a similar procedure by first propagating one of the wavefunctions to a final time when no overlap exists and then repeating the above procedure.

### *Comparison of Spectral and Pseudo-Spectral Chebychev Methods*

At this point it is appropriate to compare the Chebychev expansion of Equation 7.7 to the Newtonian interpolation formula of Equation 4.10. The connection can be worked out from Equation 7.3 by replacing the analytic integration with a Gauss-Chebychev quadrature of order  $N$ :

$$\bar{b}_n \approx \frac{2}{\pi} \sum_{l=0}^{N-1} f(z_l) T_n(x_l). \quad 7.33.$$

The quadrature points  $x_l$  are the zeros of the Chebychev polynomial of degree  $N+1$ . On inserting Equation 7.33 into the Chebychev expansion (Equation 7.7), one finds that the Chebychev expansion becomes a polynomial interpolation formula equivalent to Equation 5.9, where the quadrature points are identical to the interpolation points:

$$\begin{aligned} \sum_{n=0}^{N-1} \bar{b}_n T_n(x_k) &= \frac{2}{\pi} \sum_{n=0}^{N-1} \sum_{l=0}^{N-1} f(x_l) T_n(x_l) T_n(x_k) \\ &= \sum_{l=0}^{N-1} f(x_l) \frac{2}{\pi} \sum_{n=0}^{N-1} T_n(x_l) T_n(x_k) = f(x_k). \end{aligned} \quad 7.34.$$

The last equation is due to changing the order of summation and the Christoffel-Darboux formula (35). Another specific proof for the Chebychev polynomials is based on the substitution  $x_l = \cos \theta_l$  and  $T_n(\cos \theta) = \cos n\theta$ . From Equation 7.34, one can conclude that the Chebychev expansion of Equation 7.33 is equivalent to a polynomial interpolation when the sampling points are the zeros of the  $N+1$  Chebychev polynomial and the expansion coefficients are calculated by using the Gauss-Chebychev quadrature scheme of order  $N$ . The sampling points become the quadrature points of the numerical integration. This result means that for applications where high-order polynomial expansions are used, the Newtonian pseudo-spectral and the spectral method are equivalent. The advantage of the Newtonian method is that it is more flexible in choosing functions and interpolation points.

## PROPAGATORS FOR EXPLICITLY TIME-DEPENDENT OPERATORS

In many physical applications, the generating operator is explicitly time dependent. As an example, consider an atom or a molecule in a high-intensity laser field (59–61). The Hamiltonian of the system can be con-

sidered as containing a time-dependent part that specifically depends on the gauge chosen. Another use of an explicitly time-dependent operation is in the application of the interaction representation (24, 62). A more complicated case is in the time-dependent Hartree approach or time-dependent self-consistent field (TDSCF) methods (63, 63a) because the resulting coupled equations are nonlinear as well as time dependent. The common solution for propagation in these explicitly time-dependent problems is to use very small time steps such that within each step the Hamiltonian  $\hat{\mathbf{H}}(t)$  is almost stationary. Then one can use one of the short time propagation methods described above. A more precise approach can be obtained by considering the Magnus (64–66) expansion of the evolution operator:

$$\hat{\mathbf{U}}(t, 0) = e^{-(i/\hbar) \int_0^t dt' \hat{\mathbf{H}}(t')} - \frac{1}{2\hbar^2} \int_0^t \int_0^{t'} dt' dt'' [\hat{\mathbf{H}}(t'), \hat{\mathbf{H}}(t'')] + \dots \quad 8.1.$$

Considering the common application in which the potential is time dependent, the error in using a stationary Hamiltonian can be estimated by the second term in the Magnus series, thus leading to error  $\approx \langle \psi | [\hat{\mathbf{V}}(t), \hat{\mathbf{P}}^2] | \psi \rangle \Delta t^2$ . This means that these methods are first order with respect to the time-ordering error (22). Therefore, it is almost always advantageous to propagate with a partially time-ordered operator defined by (22)

$$\hat{\mathbf{O}} = \frac{1}{\Delta t} \int_0^{\Delta t} dt' \hat{\mathbf{H}}(t') - \frac{1}{2\hbar^2} \int_0^{\Delta t} \int_0^{t'} dt' dt'' [\hat{\mathbf{H}}(t'), \hat{\mathbf{H}}(t'')]. \quad 8.2.$$

Even for nonlinear problems where the estimation of Equation 8.2 is not explicit, it is advantageous to use the second-order correction by employing a predictor-corrector approach to estimate the commutator. In a Krylov propagation method developed explicitly for the interaction representation, the commutator can be calculated within the Krylov base (62). The short time methods lend themselves naturally to the use of variable time steps (23) whose size is adjusted to the commutator error.

In contrast to the local in-time approach, a global method has been developed to use very high order polynomial expansions (67, 68). This is done by embedding the Hilbert space of the system in a larger Hilbert space that contains an extra  $t'$  coordinate. The relation between the embedded wavefunction and the usual one subject to an initial state  $\Psi(x, 0)$  is defined as

$$\Psi(x, t) = \int_{-\infty}^{\infty} dt' \delta(t' - t) \Phi(x, t', t), \quad 8.3.$$

where  $t'$  acts like an additional coordinate in the generalized Hilbert space (69) and  $\Phi(x, t', t)$  is the solution of the time-dependent Schrödinger equation represented by the  $(t, t')$  formalism,

$$i\hbar \frac{\partial}{\partial t} \Phi(x, t', t) = \mathcal{H}(x, t') \Phi(x, t', t). \quad 8.4.$$

The  $\mathcal{H}(x, t')$  operator is defined for a general time dependent Hamiltonian by,

$$\mathcal{H}(x, t') = \hat{\mathbf{H}}(x, t') - i\hbar \frac{\partial}{\partial t'}. \quad 8.5.$$

Pfifer & Levine (70) used the time-ordering operator to give a proof of Equation 8.3; an alternative simple proof was derived by Peskin & Moiseyev (67). As Peskin & Moiseyev (67) demonstrated, the fact that  $\mathcal{H}(x, t')$  is time (i.e.  $t$ ) independent implies that the time-dependent solution of Equation 8.4 is given by

$$\Phi(x, t', t) = \hat{\mathbf{U}}(x, t', t) \Psi(x, t_0),$$

where

$$\hat{\mathbf{U}}(x, t', t) = e^{-(i/\hbar)\mathcal{H}(x, t')t}. \quad 8.6.$$

Equation 8.6 can be solved by a high-order polynomial propagator with the Newtonian or spectral method by employing the Hamiltonian (Equation 8.5) to generate the elementary mapping (68). The derivative in  $t'$  can be calculated with the Fourier method. The method is able to propagate explicitly driven systems by very high-order polynomials for extremely long times. As expected, exponential convergence was obtained. The drawback of the method is the extra degree of freedom added to solve the problem of time ordering. This extra effort is more than compensated by the added accuracy and efficiency.

## DISCUSSION

The step taken in this review to separate the methods from the application has its drawbacks because the applications usually drive the development. An important addition to the propagation methods is the ability to solve nonhomogeneous equations (6). The method has been developed for time-dependent reactive scattering in which projection operators are used to separate the asymptotic part from the interaction region. Consider the nonhomogeneous equation

$$i\hbar \frac{\partial \psi(t)}{\partial t} = \hat{\mathbf{H}}_0 \psi(t) + \hat{\mathbf{H}}_1 \chi(t). \quad 9.1.$$

It can be solved by transforming to the homogeneous form,

$$i\hbar \frac{\partial}{\partial t} \begin{pmatrix} \chi \\ \psi \end{pmatrix} = \begin{pmatrix} \hat{\mathbf{H}}_g & 0 \\ \hat{\mathbf{H}}_1 & \hat{\mathbf{H}}_0 \end{pmatrix} \begin{pmatrix} \chi \\ \psi \end{pmatrix}, \quad 9.2.$$

where  $\hat{\mathbf{H}}_g$  is the generator of the  $\chi$  motion. In this form, the polynomial expansions discussed above are applicable.

This review has overlooked an important family of nonpolynomial propagators, the split operator family. This family splits the exponential function of an operator into products of the exponentials of non-commuting operators:  $e^{\hat{\mathbf{O}}_1 + \hat{\mathbf{O}}_2} \approx e^{\alpha_1 \hat{\mathbf{O}}_1} e^{\beta_1 \hat{\mathbf{O}}_2} \dots e^{\alpha_N \hat{\mathbf{O}}_1} e^{\beta_N \hat{\mathbf{O}}_2}$ , where  $\alpha$  and  $\beta$  are determined to match the Magnus or Dyson expansion up to a particular order. The method has been introduced into molecular dynamics by Feit et al (71) who have developed a second-order version. Higher order versions have since been developed (72–74, 74a). Because of the limited scope of this review a full analysis has not been carried out, but considering high-order versions and their ability to overcome the time ordering problem (73), these methods do deserve attention. Variants of the split operator method have been developed, for example, the modified Cayley method, which is based on the expansions  $e^{\alpha_k \hat{\mathbf{O}}_1} \approx [1 - \alpha_k \hat{\mathbf{O}}_1]^{-1}$  and  $e^{\alpha_k \hat{\mathbf{O}}_1} \approx [1 + \alpha_k \hat{\mathbf{O}}_1]$  (75). Other propagation methods have been used, for example, the Crank-Nicolson method (2, 2a, 23) or the symplectic method (76). The common feature of these methods is a low-order, short-time approximation of the evolution operator.

An overview of the developments of propagator methods leads to the conclusion that high-order polynomial approximations are usually superior. Consider the evolution operator as an example. Subdividing it into short segments and using short-time, low-order expansions leads to methods that are bound to accumulate errors. If the method is unitary, the errors accumulate in the phase of the wavefunction, thus masking the quantum interference effects. Global propagators with proper stability considerations can, on the other hand, exhibit exponential convergence, thus eliminating the accumulation of errors. At this point in the development, the uniform approach has been found to be superior. The reason is that the nonuniform approaches have stability problems that severely limit the order of the expansion. Nonuniform approaches would seem advantageous for problems in which the spectral range of the operator  $\hat{\mathbf{O}}$  is very large and the initial vector  $\psi$  is supported by only a very limited part of this range. The superiority of the uniform methods is not true for

all types of propagators. The Lanczos RRGGM method (19) is able to calculate effectively correlation functions such as the survival probability  $\langle \psi(0) | \psi(t) \rangle$  (77–79). In this case, the RRGGM method is able to use a very high-order expansion of the order  $N \approx 2000$ , thus confirming the finding that when high-order expansions are used they lead to effective methods.

Finally, comparing the spectral and pseudo-spectral uniform propagators, they share the same high quality. The advantage of the pseudo-spectral method is that it is more adaptive to changing the function  $f$  and the sampling points.

### *Conclusions*

The purpose of this review is to cover an important aspect of quantum molecular dynamics, i.e. the propagation methods. In many applications, important insight has been obtained with unoptimal propagators for the task. But facing the challenge of molecular encounters in their full multidimensional glory, the representation schemes and the propagation methods have to be well optimized. One may ask: What are the trends that lead to optimized methods? In the field of representation, there is a definite movement to global  $L_2$  schemes. Spectral and pseudo-spectral representation schemes with their exponential convergence are replacing cruder semilocal representation schemes. Judging from the work covered in this review, a similar tendency seems to be emerging for propagation methods. Global methods with high-order polynomial expansions are superior, in accuracy and efficiency, to low-order short-time propagators. It seems that the nonlocal characteristic of quantum mechanics has to be reflected in the approximation schemes and that global functional representations are required for both the position-momentum phase space and the time-energy phase space.

### ACKNOWLEDGMENTS

I wish to thank my colleagues, Hillel Tal-Ezer, Charly Cerjan, David Tannor, Mark Ratner, Claude Leforestier, Rich Friesner, Nimrod Moiseyev, William Miller, Don Kouri, Stephan Gray and Daniel Neuhauser for their contributions to this work, and to my students Roi Baer, Allon Bartana, Meli Naphcha, Eyal Fatal, Uri Psekin Nir Ben-Tal, Rob Bisseling, and Audrey Dell Hammerich. This research was supported by the Binational United States–Israel Science Foundation. The Fritz Haber Research Center is supported by the Minerva Gesellschaft für die Forschung, GmbH München, FRG.

Any Annual Review chapter, as well as any article cited in an Annual Review chapter, may be purchased from Annual Reviews Preprints and Reprints service.  
1-800-347-8007; 415-259-5017; email: arpr@class.org

Literature Cited

1. Tal-Ezer H, Kosloff R. 1984. *J. Chem. Phys.* 81: 3967-70
2. McCullough EA, Wyatt RE. 1969. *J. Chem. Phys.* 51: 1253-54
- 2a. McCullough EA, Wyatt RE. 1971. *J. Chem. Phys.* 54: 3578-91
3. Kullander K, ed. 1991. *Comp. Phys. Commun.* 63: 1-584
4. Broeckhove J, Lathouwers L, eds. 1992. *Time Dependent Quantum Molecular Dynamics, NATO ASI Ser. B* 299. New York: Plenum
5. Neuhauser D, Baer M, Judson RS, Kouri DJ. 1991. *Comp. Phys. Commun.* 63: 460-72
6. Neuhauser D. 1992. *Chem. Phys. Lett.* 200: 173-78
7. Auerbach SM, Leforestier C. 1994. *Comp. Phys. Commun.* 78: 55-66
8. Auerbach SM, Miller WH. 1994. *J. Chem. Phys.* 100: 1103-12
9. Huang Y, Zhu W, Kouri DJ, Hoffman DK. 1993. *Chem. Phys. Lett.* 206: 96-102
- 9a. Zhu W, Huang Y, Kouri DJ, Anold M, Hoffman DK. 1994. *Phys. Rev. Lett.* 72: 1310-13
10. Huang Y, Zhu W, Kouri DJ, Hoffman DK. 1993. *Chem. Phys. Lett.* 214: 451-55
11. Kosloff R, Tal-Ezer H. 1986. *Chem. Phys. Lett.* 127: 223-30
12. Neuhauser D. 1990. *J. Chem. Phys.* 93: 2611-16
- 12a. Neuhauser D. 1994. *J. Chem. Phys.* In press
13. Kosloff R. 1988. *J. Phys. Chem.* 92: 2087-100
14. Hartke B, Kosloff R, Ruhman S. 1989. *Chem. Phys. Lett.* 158: 238-43
15. Baer R, Kosloff R. 1992. *Chem. Phys. Lett.* 200: 183-91
16. Lanczos C. 1950. *J. Res. Natl. Bur. Stand.* 45: 255
17. Moro G, Freed JH. 1981. *J. Chem. Phys.* 74: 3757-73
18. Köppel H, Cederbaum LS, Domcke W. 1982. *J. Chem. Phys.* 77: 2014-22
19. Nauts A, Wyatt RE. 1983. *Phys. Rev. Lett.* 51: 2238-41
- 19a. Wyatt RE. 1989. *Adv. Chem. Phys.* 73: 231-97
20. Park TJ, Light JC. 1986. *J. Chem. Phys.* 85: 5871-76
21. Leforestier C, Bisseling R, Cerjan C, Feit M, Friesner R, et al. 1991. *J. Comp. Phys.* 94: 59-80
22. Tal-Ezer H, Kosloff R, Cerjan C. 1992. *J. Comp. Phys.* 100: 179-87
23. Cerjan C, Kosloff R. 1993. *Phys. Rev. A* 47: 1852-60
24. Williams CJ, Qian J, Tannor DJ. 1991. *J. Chem. Phys.* 95: 1721-37
25. Berman M, Kosloff R, Tal-Ezer H. 1992. *J. Phys. A* 25: 1283-1307
26. Kosloff R. 1992. See Ref. 4, p. 97
27. Kosloff R. 1993. See Ref. 33, pp. 175-93
28. Gottlieb D, Orszag SA. 1977. *Numerical Analysis of Spectral Methods: Theory and Applications*. Philadelphia: SIAM
29. Kosloff D, Kosloff R. 1983. *J. Comp. Phys.* 52: 35-53
30. Harris DO, Engerholm GG, Gwinn WD. 1985. *J. Chem. Phys.* 43: 1515-17
31. Dickinson AS, Certain PR. 1968. *J. Chem. Phys.* 49: 4209-11
32. Light JC, Hamilton IP, Lill JV. 1985. *J. Chem. Phys.* 82: 1400-9
33. Cerjan C, ed. 1993. *Numerical Grid Methods and Their Application to Schrödinger's Equation, NATO ASI Ser. C* 412. Kluwer: Academic
34. Yakowitz S, Szidarovsky F. 1989. *An Introduction to Numerical Computation*, pp. 142-45. New York: Macmillan
35. Abramowitz A, Stegun IA. 1972. *Handbook of Mathematical Functions with Formulas, Graphs and Mathematical Tables*. New York: Wiley
36. Deleted in proof
37. Hammerich AD, Muga JG, Kosloff R. 1989. *Isr. J. Chem.* 29: 461-71
38. Leforestier C, Wyatt RE. 1983. *J. Chem. Phys.* 78: 2334-44
39. Kosloff R, Kosloff D. 1986. *J. Comp. Phys.* 63: 363-76
40. Neuhauser D, Baer M. 1989. *J. Chem. Phys.* 90: 4351-55
41. Child MS. 1991. *Mol. Phys.* 72: 89-93
42. Vibok A, Balint-Kurti GG. 1992. *J. Phys. Chem.* 96: 7615-22
43. Balint-Kurti GG, Vibok A. 1993. See Ref. 33, pp. 195-205
44. MacCurdy CW, Stround CK. 1990. *Comp. Phys. Commun.* 63: 323-30

45. Moiseyev N. 1991. *Isr. J. Chem.* 31: 311–22
- 45a. Reinhardt WP. 1982. *Annu. Rev. Phys. Chem.* 33: 223
- 45b. Ho YK. 1983. *Phys Rep.* 99: 1–67
46. Trefethen LM. 1980. *J. Sci. Stat. Comput.* 1: 82–102
47. Alicki R, Landi K. 1987. *Quantum Dynamical Semigroups and Applications*. Berlin: Springer-Verlag
48. Bartana A, Kosloff R, Tannor D. 1993. *J. Chem Phys.* 99: 196–210
49. Miller WH. 1972. *J. Chem. Phys.* 61: 1823–34
50. Seideman T, Miller WH. 1992. *J. Chem. Phys.* 96: 4412–22
51. Gray SK. 1992. *J. Chem. Phys.* 96: 6543–54
52. Deleted in proof
53. Pollard WT, Friesner RA. 1994. *J. Chem. Phys.* 100: 5054–65
54. Agmon N, Kosloff R. 1987. *J. Phys. Chem.* 91: 1988–96
55. Kohen D, Tannor DJ. 1993. *J. Chem. Phys.* 98: 3168–78
56. Ben-Tal N, Moiseyev N, Kosloff R. 1993. *Phys. Rev. A* 48: 2437–42
57. Zhu W, Huang Y, Kouri DJ, Chandler C, Hoffman DK. 1994. *Chem. Phys. Lett.* 217: 73–79
58. Wicks D, Tannor D. 1993. *Chem. Phys. Lett.* 207: 301–08
59. Eberly JH, Javanainen SuQ. 1989. *Phys. Rev. Lett.* 62: 881–83
60. Kulander KC, Shore BW. 1989. *Phys. Rev. Lett.* 62: 524–26;
61. Hammerich AD, Kosloff R, Ratner M. 1992. *J. Chem. Phys.* 97: 6410–31
62. Tannor DJ, Besprozvannaya A, Williams CJ. 1992. *J. Chem. Phys.* 96: 3234–39
63. Meyer HD, Manthe U, Cederbaum LS. 1993. See Ref. 33, p. 141
- 63a. Alimi R, Gerber RB, Hammerich AD, Kosloff R, Ratner M. 1990. *J. Chem. Phys.* 93: 6484–90
64. Magnus W. 1957. *Commun. Pure Appl. Math.* 7: 649
- 64a. Levine RD. 1969. *Quantum Mechanics of Molecular Rate Processes*. Oxford: Oxford Univ. Press
65. Pechukas P, Light JC. 1966. *J. Chem. Phys.* 44: 3897–12
66. Salzman MR. 1986. *J. Chem. Phys.* 85: 4605–13
67. Peskin U, Moiseyev N. 1993. *J. Chem. Phys.* 99: 4590–96
68. Peskin U, Moiseyev N, Kosloff R. 1994. *J. Chem. Phys.* 101: In press
69. Howland JS. 1974. *Math. Ann.* 207: 315–19
70. Pfifer P, Levine RD. 1983. *J. Chem. Phys.* 79: 5512–19
71. Feit MD, Fleck JA, Steiger A. 1982. *J. Comp. Phys.* 47: 412–33
72. De Raedt H. 1987. *Comput. Phys. Rep.* 7: 1–72
73. Takahashi K, Ikeda K. 1993. *J. Chem. Phys.* 99: 8680–94
74. Bandrauk AD, Shen H. 1991. *Chem. Phys. Lett.* 176: 428–31
- 74a. Bandrauk AD, Shen H. 1993. *J. Chem. Phys.* 99: 1185–93
75. Sharafeddin OA, Kouri DJ, Judson R, Hoffman DK. 1992. *J. Chem. Phys.* 96: 5039–46
76. Gray SK, Verosky JM. 1994. *J. Chem. Phys.* 100: 5011–22
77. Iung C, Leforestier C. 1992. *J. Chem. Phys.* 97: 2481–89
78. Wyatt RE, Iung C, Leforestier C. 1992. *J. Chem. Phys.* 97: 3458–86
79. Iung C, Leforestier C, Wyatt RE. 1993. *J. Chem. Phys.* 98: 6722–34